Simulation of Stress-Optic Microresonator Modulator

Jiazhao He[1], Mingjian You[1], Zhenyu Liu[1], Zhengqi Li[1], Weiren Cheng[1], Ning Ding[1], Xingyu Tang[1], Jiaxin Hou[1], and Qiancheng Zhao[1*]
[1]School of Microelectronics, MOE Engineering Research Center of Integrated Circuits for Next Generation Communications, Southern University of Science and Technology, Shenzhen, Guangdong 518000, China
[*]zhaoqc@sustech.edu.cn

Abstract

Recently there's a surge in developing piezoelectric actuated optical modulators based on the stress-optic effect. The modeling of the stress-optic microresonators requires deep understanding in photonics, solid mechanics, and electrostatics. However, it faces challenges due to the complex device structures and multi-physical interactions. In this paper, we present a modeling procedure to numerically simulate a stress-optic microresonator modulator. The ring modulator has a radius of 118 μm and a cross-section of 1.8 μm × 0.8 μm. The piezo-actuation function is enabled by 100 nm Al/1 μm AlN/100 nm Mo film stack. The resonant frequency is firstly identified by solving the azimuthal mode number, and subsequently altered by applying external voltages between the Al and Mo layers, leading to a voltage-driven frequency detuning. The simulated modulation efficiency is 0.0257 pm/V, matching well with the experimental results. This modeling approach provides a valuable tool for rapid designing and optimizing the piezo-actuated microresonator modulators.

Keyword: Piezoelectric, Stress-Optic Effect, Microresonator, Optical Modulator

Introduction

Photonic integrated circuits (PIC) play important roles in contemporary optical communication systems. Incorporating functional materials into PICs equips passive photonic devices with active modulation capabilities, unleashing great potentials in optical signal processing, quantum information computing, radio frequency synthesizing, and laser frequency stabilization. Thanks to the advances in Micro-Electro-Mechanical Systems (MEMS) [1], there is a thrust in developing piezoelectric actuated optical modulators based on stress-optic effect recently [2], [3], [4]. It involves heterogeneous integration of piezoelectric material and electrodes with optical microresonators. Such a device needs the interplay between photonics, solid mechanics, and material science. The complexity of multi-physics hinders the numerical modeling of the devices. Despite several successful experimental demonstrations, there, however, lacks a systematic procedure in designing and optimizing the piezo-actuated stress-optic microresonator modulators.

In this work, we developed a multiphysics modeling approach to simulate the piezoelectric optical modulator by using COMSOL Multiphysics®. We adopt the structure geometry from Ref. [2] as an example, as shown in Fig. 1. Next, we explain the modeling procedure and unveil the mechanism behind the multiphysics interactions. We extract the modulation efficiency from the slope of the curve of the resonant frequency versus the applied voltage, yielding a modulation efficiency of 0.0257 pm/V. The simulated results match well with the experimental data. The accuracy of the model proves its usefulness in validating the stress-optic modulators design, demonstrating its greater potential in facilitating designers for rapid designing and prototyping.

Numerical Model

As shown in Fig. 1, a microresonator modulator to be simulated is composed of the waveguide region and the piezoelectric region. The Si_3N_4 resonator has a waveguide cross-section of 1.8 μm × 0.8 μm and a radius of 118 μm. The top SiO_2 cladding is 2.4 μm-thick. On top of the waveguide cladding layer sits a piezo-electric actuator which is composed of 100 nm Mo/1 μm AlN/100 nm Al film stack from bottom to top. The model is constructed in a 2D axial symmetry structure to reduce the computational efforts while capturing the full 3D behavior of the device.

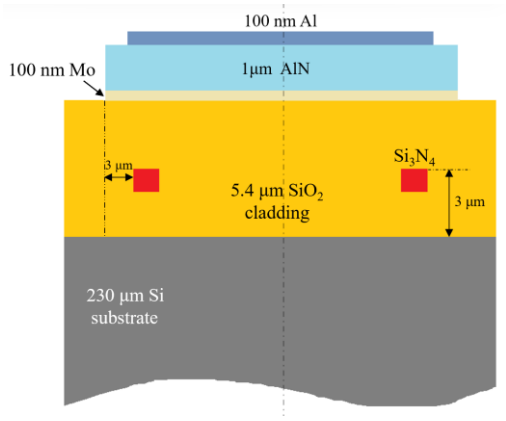

Fig. 1 The cross-section of piezoelectric optical modulator.

Mode analysis is carried out first to obtain the waveguide's fundamental TE mode profile and its effective mode index (n_{eff}) at 1550 nm. The mode profile is depicted in Fig. 2. The azimuthal mode number (m) of the resonant mode can be derived once the effective mode index is known:

$$2\pi R n_{\text{eff}} = m\lambda \tag{1}$$

The calculated m is then fed into the *Electromagnetic Wave, Frequency Domain (emw)* to track the specific resonance mode. In our case, we focus on the resonance mode of m = 879 near the resonant wavelength 1550 nm.

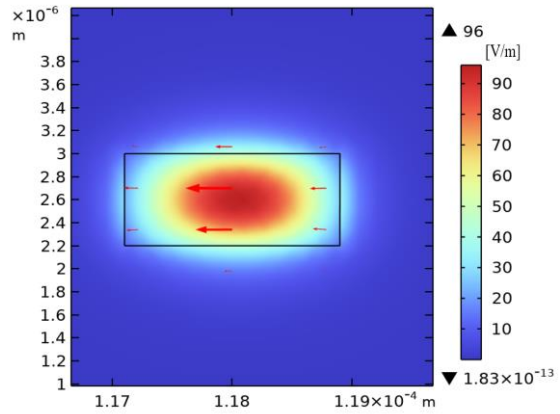

Fig. 2 The colormap shows the normalized electric field, and the arrow shows the electric field vector.

The materials' refractive indices are defined by using the *variables* in COMSOL which include the stress-optic effect [2]:

$$n_{\text{r}} = n_0 - C_1\sigma_{\text{r}} - C_2(\sigma_\varphi + \sigma_{\text{z}}) \tag{2}$$
$$n_\varphi = n_0 - C_1\sigma_\varphi - C_2(\sigma_{\text{z}} + \sigma_{\text{r}}) \tag{3}$$
$$n_{\text{z}} = n_0 - C_1\sigma_{\text{z}} - C_2(\sigma_{\text{r}} + \sigma_\varphi) \tag{4}$$

where n is the refractive index of the corresponding direction, n_0 is the materials' refractive indices without any stress applied, σ is the stress, C_1 and C_2 are first and second stress optical coefficient, r, φ, z are the spatial vectors in the cylindrical coordinate. The parameters used in the model are listed in Table 1.

Table 1 Material properties employed in stress-optic simulation

Parameter	Value	References
$n_{0,\text{Si}_3\text{N}_4}$	1.99	[5]
$C_{1,\text{Si}_3\text{N}_4}$	0.65×10^{-12} [m²/N]	[6]
$C_{2,\text{Si}_3\text{N}_4}$	4.5×10^{-12} [m²/N]	[6]

The stress on the device is produced by the AlN layer which is modeled as a stress-charge form piezoelectric material. When the piezoelectric material is forced by the mechanical stress, it generates a temporary electricity which is referred as direct piezoelectric effect. On the contrary, when the external voltage is applied, the materials will be deformed, which is called the converse piezoelectric effect [7]. The direct and converse piezoelectric effects are included in the simulation model to generate the stress from applied voltages [8]:

$$T = c_{\text{E}}S - e^{\text{T}} \tag{5}$$
$$D = eS + \epsilon_0\epsilon_{\text{rs}}E \tag{6}$$

where c_{E}, e are material properties correspond to the material stiffness, coupling properties [8], T is the stress, S is the strain, D is the electric displacement field, and E is the electric field. The coefficients are listed in Table 2.

Table 2 Material properties employed in piezoelectric simulation

Parameter	Value	Ref
e_{AlN} [C/m²]	$\begin{bmatrix} 0 & 0 & 0 & 0 & -0.48 & 0 \\ 0 & 0 & 0 & -0.48 & 0 & 0 \\ -0.58 & -0.58 & 1.55 & 0 & 0 & 0 \end{bmatrix}$	[7], [9]
$c_{\text{E,AlN}}$ [GPa]	$\begin{bmatrix} 410 & 140 & 100 & 0 & 0 & 0 \\ 140 & 410 & 100 & 0 & 0 & 0 \\ 100 & 100 & 390 & 0 & 0 & 0 \\ 0 & 0 & 0 & 120 & 0 & 0 \\ 0 & 0 & 0 & 0 & 120 & 0 \\ 0 & 0 & 0 & 0 & 0 & 130.5 \end{bmatrix}$	[7], [8]
$\epsilon_{\text{rs,AlN}}$	8.5	[7]

By using the *Electrostatics* and *Solid Mechanics* modules, the mechanical stress is simulated by applying the voltage between the top Al layer and the bottom Mo layer. Fig. 3 shows the distribution of the z component of the stress on the device.

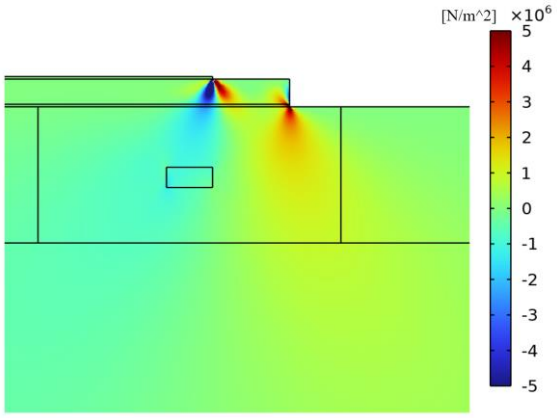

Fig. 3 The distribution of the z component of the stress tensor at 60 V bias voltage.

The piezoelectric effect induced stress leads to structure deformation, assuming the device has a fixed constraint on the outer edge and the bottom of the disc, with free boundary elsewhere. The deformed structure is illustrated in Fig. 4.

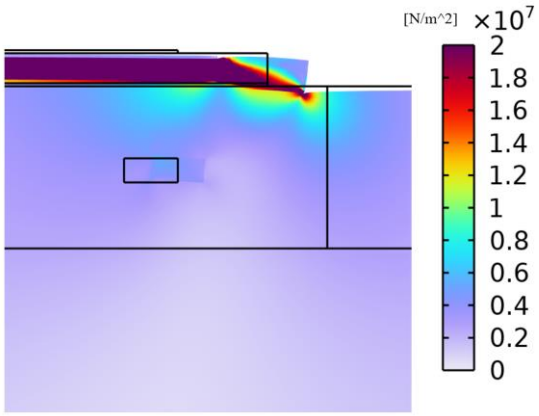

Fig. 4 the displacement shows deformation of the device, scale factor =1000, and the colormap shows the von-mises stress on the device.

Results

Given the applied external voltage and the induced mechanical stress, the effective mode index of the guided mode is altered, resulting in a detuning of the resonant frequency. We sweep the applied voltage across the Al and the Mo layers. The resonant frequency at the fixed azimuthal mode number is correspondingly solved at each voltage. Fig. 5 shows that the resonant wavelength and resonant frequency shift with respect to the external voltage, revealing the modulation effect on the resonant condition. The modulation efficiency is extracted from the slope of the curve and is estimated to be 0.0257 pm/V. The simulation results of the model match well with the experimental results (about 0.02 pm/V) [6], which shows the high accuracy of the model.

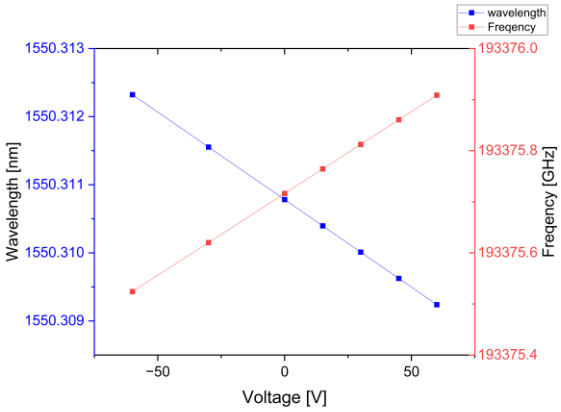

Fig. 5 The resonant wavelength (left axis) and the resonant frequency (right axis) as functions of the bias voltages.

Conclusion

The demonstrated simulation procedure provides a useful approach to accurately model and analyze the performance of piezo-actuated heterogeneously integrated microresonator modulators, which will not only contribute to a better understanding of the expected performance but also simplifies the design process and improve the production yield.

Reference

[1] L. Midolo, A. Schliesser, and A. Fiore, “Nano-opto-electro-mechanical systems,” *Nature Nanotechnology*, vol. 13, no. 1, pp. 11–18, Jan. 2018, doi: 10.1038/s41565-017-0039-1.

[2] H. Tian *et al.*, “Hybrid integrated photonics using bulk acoustic resonators,” *Nature Communications*, vol. 11, no. 1, p. 3073, Jun. 2020, doi: 10.1038/s41467-020-16812-6.

[3] J. Wang, K. Liu, M. W. Harrington, R. Q. Rudy, and D. J. Blumenthal, “Silicon nitride stress-optic microresonator modulator for optical control applications,” *Opt. Express*, vol. 30, no. 18, pp. 31816–31827, Aug. 2022, doi: 10.1364/OE.467721.

[4] P. R. Stanfield, A. J. Leenheer, C. P. Michael, R. Sims, and M. Eichenfield, “CMOS-compatible, piezo-optomechanically tunable photonics for visible wavelengths and cryogenic temperatures,” *Opt. Express*, vol. 27, no. 20, pp. 28588–28605, Sep. 2019, doi: 10.1364/OE.27.028588.

[5] Q. Zhao *et al.*, “Low-loss low thermo-optic coefficient Ta2O5 on crystal quartz planar optical waveguides,” *APL Photonics*, vol. 5, no. 11, p. 116103, Nov. 2020, doi: 10.1063/5.0024743.

[6] H. Tian, “Piezoelectric transduction of Silicon Nitride photonic system,” Purdue University Graduate School. Accessed: Aug. 07, 2024. [Online]. Available: https://hammer.purdue.edu/articles/thesis/Piezoelectric_transduction_of_Silicon_Nitride_photonic_system/19669569/1

[7] G. Bu, D. Ciplys, M. Shur, L. J. Schowalter, S. Schujman, and R. Gaska, “Electromechanical coupling coefficient for surface acoustic waves in single-crystal bulk aluminum nitride,” *Applied*

Physics Letters, vol. 84, no. 23, pp. 4611–4613, Jun. 2004, doi: 10.1063/1.1755843.

[8] "Multiphysics, C. Introduction to comsol multiphysics®. https://www.comsol.com/support/knowledgebase/1223 (1998).", [Online]. Available: https://www.comsol.com/support/knowledgebase/1223

[9] M. A. Fraga, H. Furlan, R. S. Pessoa, and M. Massi, "Wide bandgap semiconductor thin films for piezoelectric and piezoresistive MEMS sensors applied at high temperatures: an overview," *Microsystem Technologies*, vol. 20, no. 1, pp. 9–21, Jan. 2014, doi: 10.1007/s00542-013-2029-z.